processes

MDPI

Article

Efficient Solutions for Electronic Chip Cooling: Multi-Objective Optimization Using Evolutionary Algorithms with Boron Nitride Nanotube-Based Nanofluid

Mohammed R. A. Alrasheed

Department of Mechanical Engineering, College of Engineering, King Saud University, P.O. Box 800, Riyadh 11421, Saudi Arabia; mohalrasheed@ksu.edu.sa

Abstract: Optimization algorithms have significantly evolved because of advancements in computational capacity. This increase aids in the availability of data to train various artificial intelligence models and can be used in optimizing solutions for electronic chip cooling. In the current study, such a microchannel heat sink (MCHS) is optimized using a Boron Nitride Nanotube (BNN)-based nanofluid as a coolant. Thermal resistance and pumping power are chosen as the objective functions, while geometric parameters such as the channel aspect and width ratio are used as the design variables. Multi-objective multiverse optimizer (MOMVO), an evolutionary algorithm, is used to optimize both objective functions, which are minimized simultaneously. The primary objective of this study is to study the applicability of such advanced multi-objective optimization algorithms, which have not previously been implemented for such a thermal design problem. Based on the study, it is found that the optimal results are obtained with a population size of only 50 and within 100 iterations. Using the MOMVO optimization, it is also observed that thermal resistance and pumping power do not vary significantly with respect to the channel aspect ratio, while pumping power varies linearly with the channel width ratio. An optimum thermal resistance of 0.0177 °C/W and pumping power of 10.65 W are obtained using the MOMVO algorithm.

Keywords: electronics cooling; geometric optimization; microchannel heat sink; multiverse optimizer; multi-objective optimization; nanofluids

Citation: Alrasheed, M.R.A. Efficient Solutions for Electronic Chip Cooling: Multi-Objective Optimization Using Evolutionary Algorithms with Boron Nitride Nanotube-Based Nanofluid. *Processes* **2023**, *11*, 3032. https://doi.org/10.3390/pr11103032

Academic Editors: Hussein A. Mohammed and Kian Jon Chua

Received: 4 September 2023
Revised: 26 September 2023
Accepted: 19 October 2023
Published: 21 October 2023

1. Introduction

The electronics industry is growing ever-increasingly due to consistent technological improvements and demand for higher computational power. This is coupled with the fact that the use of electronics is increasing in day-to-day life. However, with the increase in the computational capacity of electronics, its power consumption and dissipation also increase [1]. Moore's law, a well-known principle in electronics, states that the performance of electronic devices doubles every eighteen months. This is accompanied by an increase in transistor density and, thus, power consumption [2]. This power generation increase must be addressed by using enhanced cooling solutions without substantially increasing the cost. Thus, the design and operating parameters of these cooling systems need to be optimized. Microchannel heat sinks (MCHS), which are gaining popularity for such compact cooling solutions, have reached their peak, so these systems need to be optimized [3]. The thermal resistance and pumping power of these cooling solutions need to be considered for the MCHS to have better heat transfer and low power consumption [4,5]. Thus, multi-objective optimization needs to be carried out by suitable solvers that have high reliability and rapid convergence.

1.1. Microchannel Heat Sink

With increasing demand for cooling density, advances in liquid cooling technology, such as microchannel heat exchangers, are important. Due to the small size of the electronics,

the flow area, especially near the heat source, is generally of a very small scale, making microchannel dynamics applicable. Zhao and Lu [6] analyzed microchannel heat transfer in a heat sink for cooling electronics. They proposed analytical as well as numerical methodologies to determine the global heat transfer coefficient in the microchannel. The variations in the Nusselt number were studied with respect to the channel aspect ratio. From the analysis, it was found that the fin assumption resulted in overestimation of the heat transfer.

A comparative study by Kose et al. [7] on different shapes of microchannel heat sinks concluded that rectangular microchannel geometry was the most effective configuration in terms of both hydrodynamic and thermal performance. Jing and He [8] conducted a numerical study on three different shapes of microchannel heat sinks. They concluded that elliptical microchannels and rectangular microchannels, interchangeably, demonstrated the best hydrodynamic and thermal performance at different hydraulic diameter,. Based on these studies, we chose rectangular straight microchannels for our study. A review of the thermal and hydrodynamic analysis of microchannel heat sinks presented by Ahmed et al. [9] stated that the rectangular microchannel shape is preferred by most researchers due to its stability, ease of machining, and good thermal performance, complemented by optimal hydrodynamic performance.

Ramos-Alvarado et al. [10] carried out computational studies on a microchannel heat sink by comparing its performance with conventional cooling techniques. The study was carried out for cooling high-heat-flux entities, such as high-power electronics, fuel cells, solar cells, etc. To get a robust comparison between the microchannel and conventional cooling techniques; pumping power was also considered in the study. Eight different MCHS flow configurations were considered to determine the best flow arrangement. It was found from the study that the lowest thermal resistance and pumping power were obtained when there was a greater flow distribution in the MCHS.

Saenen and Baelmans [11] developed a comprehensive model for determining the thermal resistance of an MCHS that has multi-phase flow for a higher heat transfer rate. Transient simulations were carried out using transfer models for solids, while the SIMPLE algorithm was employed for the fluid domain. The model was validated using published results [12], so as to allow its use for future developed models.

Silvério et al. [13] addressed the demand for microchannel heat sinks integrated with the electronics itself. An experimental investigation was carried out on a microchannel heat sink embedded in a semiconducting material by varying the fin thickness and width. A heat transfer rate of 10.8 Watts per square centimeter was obtained in the single-phase operation of the heat sink. Here, the temperature of the electronic chip was successfully kept below 85 °C when the coolant flow rate was 3 LPH. For the same MCHS, the heat flux can be increased by 150% if two-phase heat transfer is employed at a flow rate that is less than 50% of the single-phase rate.

Kong et al. [14] considered thermal resistance and pressure drop when analyzing an MCHS using 3D models. Manifold heat sinks were chosen for the study, and a comparison with a conventional microchannel was undertaken. From the analysis, it was concluded that the thermal resistance was reduced by up to 50%, while the pressure was reduced by up to 90%, depending on the type of flow cross-section used.

Nemati et al. [15] used a multi-objective genetic algorithm for the optimization of an MCHS for small-scale applications. Here, the fins were formed in a wavy pattern instead of the conventional straight design. A three-dimensional simulation was carried out to determine the thermal and hydraulic performance. The study found that the thermal resistance was reduced by 87% due to the wavy fins, while the pumping power increased by merely 10%.

Yang et al. [16] considered geometric aspects while evaluating the thermal resistance and pressure drop of a manifold MCHS. It was shown that the effective heat transfer area can be increased by varying the geometric parameters of the MCHS. The thermal

performance of the MCHS was doubled while achieving an extensive high heat flux of 2500 W/m^2.

Maghrabie et al. [17] explored the use of nanofluids in the improvement of heat transfer in microchannel cooling of electronics. The effects of various aspects of nanofluids were studied to understand their effect on heat sink performance. Different heat transfer correlations were also analyzed for their application in microchannel heat transfer. The effect of surface roughness of the MCHS when using nanofluids was also highlighted.

Zhang et al. [18] studied different MCHS formats in order to reduce the temperature of high heat flux electronic chips being cooled. The heat transfer coefficient was enhanced by introducing turbulence using varying cross-sections of the bottom of the microchannel. It was concluded that zigzag cavities performed better than wavy and step cavities.

Du and Hu [19] summarized microchannel heat sinks by comparing different studies of their performance. It was shown that the increase in the power density of electronics was the driving force behind microchannel heat sink design improvements. Shen et al. [20] studied a multi-layer MCHS with a nested jet as the cooling source. It was shown that the jet not only provided cooling throughout the heat sink, but having the jet impinge at the appropriate location could help reduce the maximum temperature; it was found that the hot-spot temperature was reduced by 20 K, while the average Nusselt number increased by 5.3%.

With technological advancement in place, several researchers have attempted to optimize heat sink design by varying its design and performance parameters.

1.2. Optimization of MCHS

Marshall and Lee [21] undertook a study on the enhancement of MCHS performance using nine different topologies. The study highlighted the importance of using 3D geometry instead of 2D for better overall thermal performance. The improvement was attributed to the change in the fluid flow parameters across the height of the heat sink.

Ozguc et al. [22] carried out topological optimization of an MCHS, which could be operated dynamically. The heat sink was optimized for electronics with different hot spots by introducing gates for individual hot spots. The gates opened and closed according to the status of these hot spots, resulting in efficient utilization of the fluid flow. Using Pareto curves, the thermal performance of two different heat sinks improved by 10.7% and 6.8%, respectively.

Shuqi et al. [23] used neural networks to optimize the baffles used in the MCHS for optimum flow distribution. Here, the Nusselt number was chosen as the optimization function, which was optimized by varying the distance between the baffles. The study found that the vertical distance between the baffles had a maximum influence on MCHS performance. This was the result of better flow distribution when the vertical distance between baffles was higher.

Tan et al. [24] optimized the structural design of the MCHS by using the combined thermal and hydraulic performance. The study included the entire set of heat sink parameters instead of only the microchannel for a more robust performance. A genetic algorithm was used to determine the optimum parameters, and it was found that the microchannel parameters were the most influential on the thermal as well as hydraulic performance of the MCHS. Here, the pumping power was reduced by 25%, while the heat transfer increased by 20%.

Ismail et al. [25] improved the performance of an MCHS by using fins to create turbulence in the fluid flow. The structural design of the fins was optimized by assessing over 200 configurations. Similar weightage was given to thermal resistance and the pressure drop, resulting in optimum performance.

Cui et al. [26] used multi-objective optimization of an MCHS with jet impingement. Various geometric parameters of the MCHS were considered as design variables for the optimization. The multi-objective particle swarm method (PS) and genetic algorithms (GA) were used for the optimization, resulting in a heat transfer rate of 200 W/cm^2 for a minimal pumping power of 5.7 kPa.

Bianco et al. [27] carried out topological optimization of the MCHS using uniform temperature at the boundary. The theoretical average temperature was chosen as the optimization function in a finite element model. The analysis concluded that the heat removal capacity of the optimized MCHS improved by up to 100%.

Topin et al. [28] reviewed power electronics cooling and recommended that metal foam provided the best cooling solution but was difficult to use. With significant improvement in its manufacturing and integration it may be viable in the future, but it remains an engineering challenge to implement it.

Shanmugam and Maganti [29] optimized a parallel flow MCHS sink to reduce thermal resistance and pumping power. Using neural networks, optimization was carried out on a 3D-geometry heat sink. Thermal resistance of 0.0306 °C/W was obtained for a pumping power of 3.1 kPa.

Xiao et al. [30] designed, manufactured, and tested a closed-loop system combining a microchannel sink and jet impingement with R-134a as the working fluid. The study concluded that the hybrid heat sink can be used to achieve low thermal resistance, stemming from a highly dense micro-jet array with separate inflow and outflow microchannels.

1.3. Multi-Objective Multiverse Optimizer Algorithm

Abd Elaziz et al. [31] optimized a grey-scale image using the MOMVO algorithm. This algorithm was chosen because there was more than one objective, and it was desired to conduct the optimization in a single step. By comparing the results from their work over eleven scales with a wide range, it was found that a finer prediction of the Pareto Front was obtained.

Acharya et al. [32] carried out the optimization of power-generating units using the MOMVO algorithm in order to achieve the lowest cost of generation. Valve-point effects were used to reduce the dynamic load by considering its monetary value. The solver was tested using a large number of generating units, i.e., objective function, and the solver was able to provide consistent optimum results. Thus, it was concluded that the solver shows the potential to replace existing solvers, especially for multi-objective optimization.

Sundaram [33] used the MOMVO algorithm to reduce transmission losses dynamically. Artificial neural networks were incorporated in the system in order to digitize the process. Based on the results obtained by using the solver on 54 power-generating units, it was found that the solver provided consistent predictions. Compared with the GA and PS algorithms, the time taken by the proposed solver was 30 and 7.6 times faster, respectively.

Xu and Yu [34] undertook the optimization of multi-objective functions to address the pollution from fossil-fuel-based power generation units. Environmental as well as economic factors were taken into consideration while determining the dispatch problem. By comparing different popularly used multi-objective optimization algorithms, it was found that the MOMVO algorithm had better reliability, stability, and convergence for the given problem.

As can be observed from the literature, electronics cooling demand is increasing as computational power per unit volume increases. Simultaneously, the multi-objective multiverse optimizer algorithm has shown significant potential when compared with other popular multi-objective optimization methods. Not only has it shown better convergence and stability, but it has also increased the potential to incorporate more objectives into the optimization problem. Cooling of electronics has more than one objective, i.e., thermal resistance, pumping power, etc., that need to be optimized simultaneously. Faced with the increase in demand for cooling density in high-power electronics, the MOMVO algorithm can improve the performance of the cooling solution. Thus, this study uses the optimization model on the heat sink, for which a mathematical model is presented to predict its performance. Two objective functions of thermal and hydraulic performance, i.e., thermal resistance and pumping power, are optimized simultaneously using the optimization solver.

1.4. Nanofluids

The conventional fluids that are used in microchannel heat sinks are water and ethylene glycol. However, with the advancement in technology, microelectronic devices have been introduced. The heat generation of these devices has been increasing exponentially, so conventional fluids are unable to meet the increased cooling demands. To tackle this problem, a new type of fluid called a nanofluid is used to improve the cooling performance of microchannel heat sinks. A review of recent progress in nanofluid applications in microchannel heat sinks by Loon and Sidik [35] concluded that the suspension of nanoparticles in base fluid was proven to be effective for enhancing the thermal conductivity of the base fluid and improving the heat transfer performance of the microchannel heat sink. Boron nitride-based nanofluids are used in this study because they have good thermal stability, and they can be utilized to enhance the thermal conductivity of the base fluid. Gómez-Villarejo et al. [36] conducted an experimental study and found that the thermal properties of the fluids improved with the use of boron nitride-based nanoparticles without modifying the pressure drop and pumping power.

1.5. Research Gap

The literature review presented so far indicates that no optimization technique based on an evolutionary algorithm has been conducted for optimization of the thermal performance and hydrodynamic performance of an MCHS with a nanofluid coolant, though the use of nanofluids as coolants is under exploration by researchers to find new potential coolants with desired properties [35]. Specifically, the multi-objective multiverse optimizer (MOMVO) approach has never been used for this purpose. Hence, this study utilizes the MOMVO, an evolutionary algorithm, for optimization of the thermal and hydrodynamic performance of a straight MCHS with rectangular channels and BNN-based nanofluid as the coolant.

1.6. Objectives

The objectives of this study are given below:

- Investigation of the applicability of advanced multi-objective optimization algorithms, which have not previously been implemented for such a thermal design problem;
- Optimization of the thermal resistance and the pumping power of the MCHS cooled with Boron Nitride Nanotube-based nanofluids;
- Use of multi-objective multiverse optimizer (MOMVO), an evolutionary algorithm, for optimization of the thermal resistance and the pumping power;
- Determining the optimum geometric parameters for the chosen configuration of MCHS, i.e., straight, rectangular channels.

2. Design Optimization of MCHS

The thermal and hydrodynamic performance of the MCHS are optimized to extract the best output from it. To obtain the maximum heat transfer from the MCHS, the geometric parameters are optimized, and a mathematical model is developed to quantify the performance of the MCHS. The schematic of the MCHS is shown in Figure 1. The MCHS has several microchannels through which the cooling fluid flows. Here, a basic heat sink is considered to compare the performance of the MOMVO algorithm with other conventional optimization algorithms. Different geometric parameters are taken into consideration in optimizing the heat sink's performance. Here, the electronic chip that is to be cooled is in direct contact with the MCHS through a BNN nanofluid, which is used to enhance heat transfer, as reported in the literature [11].

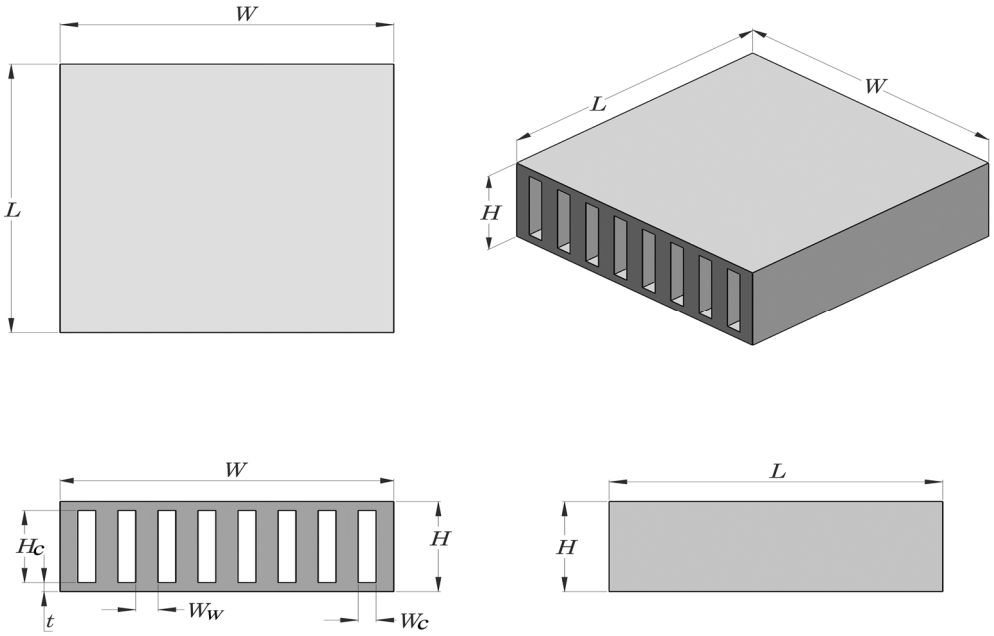

Figure 1. Microchannel heat sink.

The cooling of the electronics through cooling fluid involves complex three-dimensional interactions. Analytical solutions to such a problem involve extensive mathematics, which can be difficult to solve using conventional means. Thus, to simplify the model, some assumptions are made, as listed below. These assumptions are chosen in such a way that the accuracy of the solution is not compromised.

- The geometry is assumed to be 2D for calculations.
- Variations across the length of the MCHS are ignored.
- The fluid flow is assumed to be laminar.
- The fluid flow is assumed to be steady.
- The average temperature is assumed to be constant at 50 °C.
- The flow is fully developed and of uniform density.
- The variations in the thermophysical characteristics are one-dimensional only.
- Uniform temperature over the cross section.
- Smooth interior walls, averaged heat transfer.
- Effects of body forces are neglected.
- The channel walls are assumed to be a fin with an insulated tip.
- The geometry of the microchannel heat sink (MCHS) is taken as a cuboid with Length "L", Width "W", and Height "H". There are rectangular slit channels along the width and height plane. The height of the channel is "H_c", and the width is "W_c". The gap between the slits is "W_w".

Ideally, a three-dimensional simulation of the MCHS under study may be conducted to obtain its thermal and hydraulic performance. However, the aim of the present work is to study the performance of the MOMVO algorithm with respect to its MCHS performance. Thus, in the present work, the MOMVO algorithm is applied to a simplified mathematical model of the MCHS.

2.1. Mathematical Model

The mathematical model used to optimize the thermal resistance and pressure drop across the MCHS is presented in this section. The objective functions used for the optimization are the thermal resistance ($R_{thermal}$) and the pumping power ($P_{pumping}$).

The geometric parameters used for the study are heat sink height (H), heat sink length (L), heat sink width (W), microchannel width (W_c), microchannel height (H_c), and the width of the walls between the microchannels (W_w). These parameters are combined into different

variables in order to obtain a robust and parametric result that can be applied to a wider domain of heat sinks. The channel aspect and width ratios, α and β, are defined as given in Equation (1) below. These are used as the design variables, keeping the total height, length, and width of the MCHS constant.

$$\alpha = \frac{H_c}{W_c} \text{ and } \beta = \frac{W_w}{W_c} \tag{1}$$

The total number of microchannels (n) is defined using the heat sink width, microchannel width, and the channel width ratio as in Equation (2).

$$n = \frac{W \times \alpha}{H_c \times (1+\beta)} \tag{2}$$

To determine the flow and heat transfer characteristics of the fluid, the hydraulic diameter (D_h) is defined in Equation (3) [37]:

$$D_h = \frac{2}{1+\alpha} \times H_c \tag{3}$$

The Reynolds number is evaluated as given below in Equation (4) [37].

$$R_e = \frac{2 \times \rho_f \times G}{\mu_f \times n \times H_c} \times \frac{\alpha}{1+\alpha} \tag{4}$$

Here, G is the mass flux through the heat sink while μ_f and ρ_f are the fluid viscosity and density. The average Nusselt number is evaluated using Equation (5) [25].

$$Nu = 2.253 + 6.164 \times \left(\frac{\alpha}{1+\alpha}\right)^{1.5} \tag{5}$$

The global average heat transfer coefficient (h_{av}) is evaluated as shown in Equation (6) [38].

$$h_{av} = \frac{Nu \times k_f}{D_h} \tag{6}$$

Here, the conduction through the microchannel walls is also incorporated into the model by assuming the side walls as fins experiencing convection on their sides while having the same base temperature as that of the electronics. Here, the top of the wall is connected to the top part of the MCHS, where very little heat transfer is happening; thus, it is assumed to be adiabatic. For this condition, the fin efficiency (η) is evaluated as in [39]:

$$\eta = \frac{\tanh(mH_c)}{mh_c} \tag{7}$$

here, m is the fin parameter, calculated as,

$$m = \sqrt{\frac{2 \times h_{av} \times \alpha}{K_s \times H_c \times \beta}} \tag{8}$$

Here, K_s is the thermal conductivity of the fin material (heat sink material in the present case). Using the concept of the electrical analogy of heat transfer [39], the thermal resistance of the MCHS is defined as given in Equation (9) below.

$$R_{thermal} = \frac{2 \times L \times (1+\beta)}{C_{pnf} \times \mu_{nf} \times R_e \times (1+\alpha)} + \frac{(1+\beta)}{h_{av} \times (1+2\alpha\beta)} + \frac{t}{K_{hs}(LW)} \tag{9}$$

Similarly, in order to measure the hydrodynamic performance, first, the friction factor is calculated as given in Equation (10) [38], where *Re* is the Reynolds number.

$$f = \frac{64}{Re} \tag{10}$$

For a nanofluid, the pressure drop is evaluated using the following equation [37]:

$$\Delta P = P_1 + P_2 \tag{11}$$

where P_1 and P_2 are calculated using Equations (12) and (13) [37].

$$P_1 = f \times \frac{(1+\alpha) \times L}{2 \times H_c} \times \rho_f \times \frac{V_{mf}^2}{2} \tag{12}$$

$$P_2 = \left(1.79 - 2.23\left(\frac{1}{1+\beta}\right) + 0.53\left(\frac{1}{1+\beta}\right)^2\right) \times \rho_f \times \frac{V_{mf}^2}{2} \tag{13}$$

Here, V_{mf} is the mean velocity of the nanofluid evaluated as in Equation (14) [37]:

$$V_{mf} = \frac{Re \times \mu_f}{\rho_f \times H_c} \tag{14}$$

The pumping power is calculated using the pressure drop using Equation (15) [37], as shown below.

$$P_{pumping} = \Delta P \times G \tag{15}$$

2.2. MOMVO Algorithm

Multiverse optimization (MVO) algorithms were initially developed to obtain a better optimizer methodology. The MVO algorithm was developed using cosmological concepts. Initially, the algorithm developed was shown to have great potential when compared to conventional particle swarm and genetic algorithms. Thus, the MVO was extended to multi-objective optimization problems. For the present study, it is desired to optimize the thermal and hydraulic performance of the MCHS to achieve the optimum performance. Hence, the MOMVO algorithm is used to carry out the simultaneous minimization of both chosen objective functions.

The flow chart used for the MOMVO algorithm implementation to optimize the performance of the MCHS is shown in Figure 2. The solver takes the geometric and hydraulic properties as the initial input. As the solver is evolutionary, one initial population is generated for which the objective functions, thermal resistance and pressure drop, are identified. Using the population and their ranks, the new population is generated, which is supposed to perform better than its parent population. The main benefit of using the MOMVO algorithm is the method by which the population is mutated in the next generation, keeping in mind both the objective functions. The mutation process is repeated till the desired number of new generations is obtained.

The MOMVO algorithm was initially validated using published results [37]. From comparisons, it was found that the model was successfully able to converge to the published results with good accuracy. After developing satisfactory confidence in the model, it was applied to the MCHS as described in the present study. The details of the MOMVO algorithm criteria are given in Table 1. The design variables and the objective function are known for the present case, while the other values are determined using the literature.

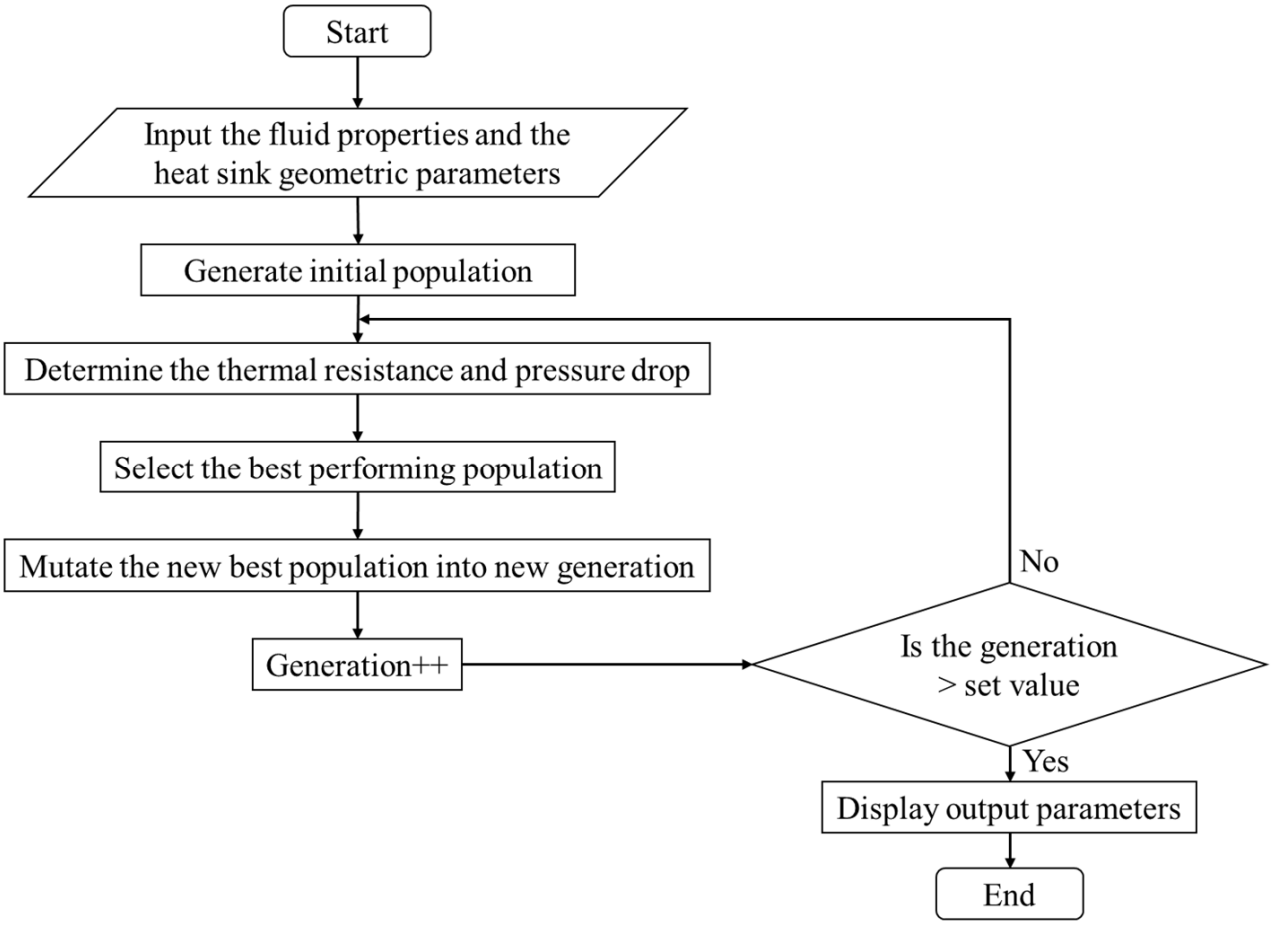

Figure 2. MOMVO optimization algorithm.

Table 1. MOMVO algorithm criteria.

Criteria	Description
Number of iterations	100
Size of the population	50
Number of variables	2
Number of objective functions	2
Number of cases	6
K_s (W/m K)	148
K_{hs} (W/m K)	170

Here, the thermal conductivity of the MCHS material and the nanofluid are taken at a constant average temperature of 50 °C. Shamsuddin et al.'s study [40] concluded that any change in thermal resistance greatly reduces the pressure drop at an optimum temperature of 50 °C. In addition, the upper and lower bounds of the design variables, i.e., the channel aspect and width ratio, are also specified. These values are considered, keeping in mind the practical limitations of the MCHS. The upper and lower bounds of the design variables are stated in Table 2.

Table 2. Upper and lower bounds of the design variables.

Bounds	α	β
Max	10	0.1
Min	1	0.01

Using the developed mathematical model and the described optimization algorithm, the design optimization is carried out on the MCHS using a BNN nanofluid for cooling electronics. The study also considers varying weights of nanoparticles in the fluid (water). The optimum thermal resistance and pumping power are obtained for all six cases, i.e., one with only water and five with varying weights of nanoparticles in the water. The details of the six different fluids are provided in Table 3, along with the relevant thermophysical properties required to carry out the optimization.

Table 3. Thermophysical properties of the six fluids used for the optimization study [37].

	Fraction of Nanoparticles in Water (wt. %)					
Fluid	**0**	**0.03**	**0.01**	**0.005**	**0.003**	**0.001**
k (W/m K)	0.567	0.566	0.577	0.595	0.596	0.56
ρ (kg/m^3)	990.2	990.4	990.5	990.7	990.9	989.8
C_p (W/kg K)	4.115	4.1513	4.1717	4.2885	4.2456	4.0041
μ (N s/m^2)	0.4942	0.49298	0.48897	0.49107	0.504	0.5051

3. Results and Discussion

Table 4 shows the thermal resistance and pumping power of the MCHS cooled with pure water, and the water with BNN nanofluids at 0.001%, 0.003%, 0.005%, 0.01%, and 0.03% by weight at 50 °C. In this study, the channel height and the volumetric flow rate were taken as 320 µm and 4.7 × 10^{-6} m^3/s, respectively. Initially, the optimization was carried out with various population sizes to understand the effect of population size on the convergence of the solver. Population sizes of 50, 100, 200, 500, and 1000 were considered, and it was found that the results were similar to each other. As the population size of 50 required fewer steps in searching for the optimum results, it was chosen for further optimizations. However, it should be kept in mind that the population should be diverse enough to capture the entire domain of search, such that the global optimum is reached rather than a local optimum. As can be seen from the table, as the percentage of nanoparticles increases in the fluid, the channel aspect ratio generally increases, with deviations for a few data points. The channel width ratio is constant for all the cases at its lowest value of 0.01. This indicates that a higher performance is obtained when the channel width ratio is lower. The thermal resistance does not vary noticeably as the nanofluid concentration varies in the fluid. However, the pumping power initially reduces and then increases. Thus, for better understanding, another parameter, which is the product of thermal resistance and pumping power, is defined as shown in the table. Here, it can be observed that this product is lowest for 0.01% of nanofluid and then increases, indicating that 0.01% nanoparticles in the fluid is the optimum concentration. By the addition of 0.01% nanofluid to the water, the thermal resistance was reduced by 1.2%, while the pressure drop was reduced by 0.22%. The product of thermal resistance and pumping power was reduced by 4.8%, which is a significant reduction.

Table 4. Optimization result for MCHS for different fluids.

Nano Particles in Fluid (% wt.)	**α (1–10)**	**β (0.01–0.1)**	**Thermal Resistance (K/W)**	**Pumping Power (W)**	**Thermal Resistance × Pumping Power**
0	1.3799859	0.01	0.0179389	11.00474	0.197413
0.001	1.3533110	0.01	0.0177926	10.76724	0.191577
0.003	1.9023564	0.01	0.0177339	10.74079	0.190476
0.005	1.1972700	0.01	0.0177248	10.65324	0.188827
0.01	1.9143233	0.01	0.0175656	10.69918	0.187938
0.03	1.3670916	0.01	0.0176264	10.98077	0.193551

The graph in Figure 3 shows the relationship between the thermal resistance and pumping power of water and BNN fluids as a result of the optimization with MOMVO. It may be noted that the curve follows a rectangular hyperbolic pattern, with both of the

objective variables on each axis. It is observed that the pumping power is very high for very low thermal resistance and vice versa, as shown by the green and blue regions, respectively. The red circle zone on the figure indicates the optimized solution where both the thermal resistance and the pumping power are low. As can be seen from the graph, the optimum point does not lie on the x = y line but on the right side of it. This indicates that the thermal resistance has a greater effect than the pressure drop on the performance of the MCHS. As a result, the optimum thermal resistance and pumping power of 0.0179 K/W and 11.00 W are obtained, respectively. Hence, the addition of nanoparticles in base fluids enhances the cooling capacity of the MCHS.

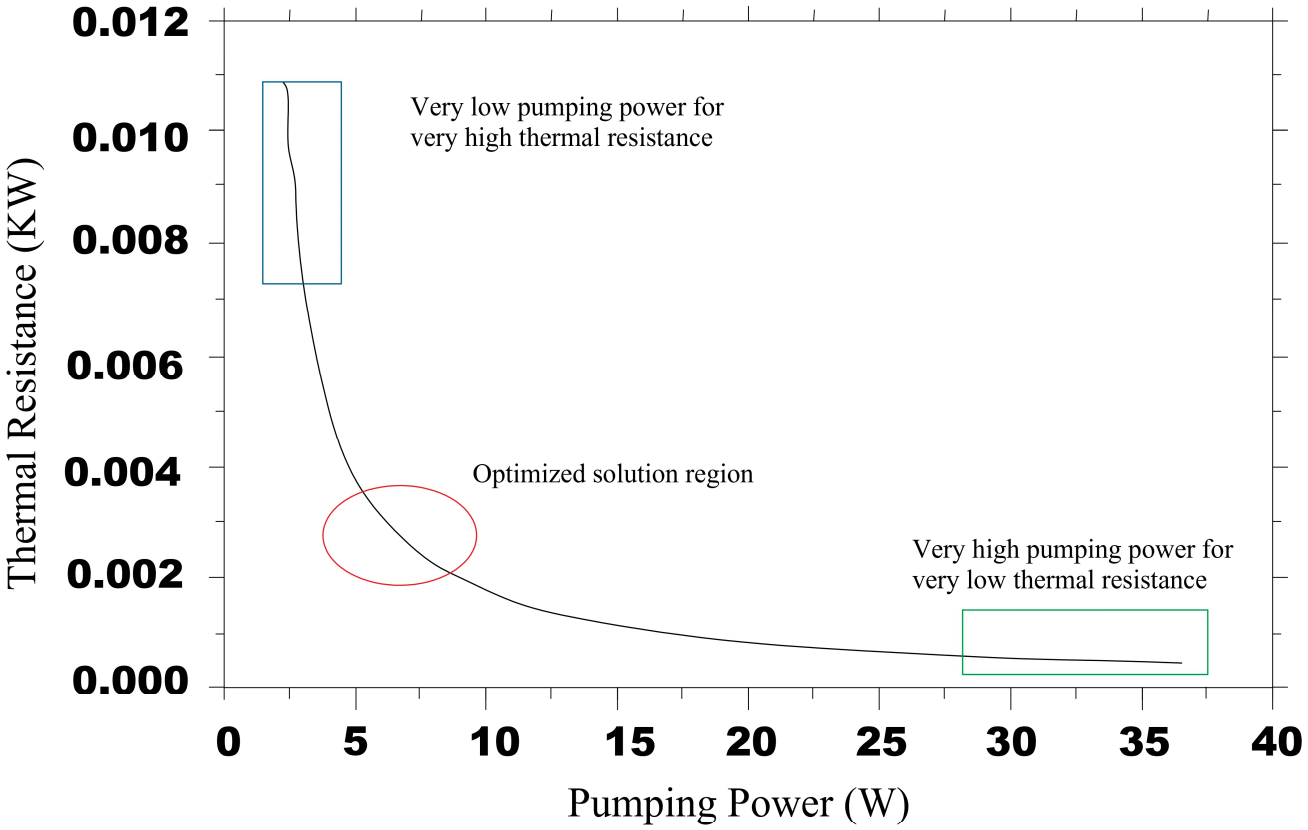

Figure 3. Optimization of BNN nanofluids for water.

The main parameters affecting the geometrical properties in this study are the channel aspect ratio, α, which is the ratio of the heat sink's channel height to channel width, and the wall width ratio, β, which is the ratio of the heat sink's wall width to channel width. These two critical parameters for optimization of thermal resistance and pumping power are kept within the limited range of values set by Table 2 to avoid incoherent results.

Figure 4 shows the variation of the thermal resistance with respect to pumping power for a channel aspect ratio of one, i.e., height and width are the same up to 10, which is decided based on practical limitations. Here, the variations are shown for water as the fluid; however, with the nanofluids, the trends are similar.

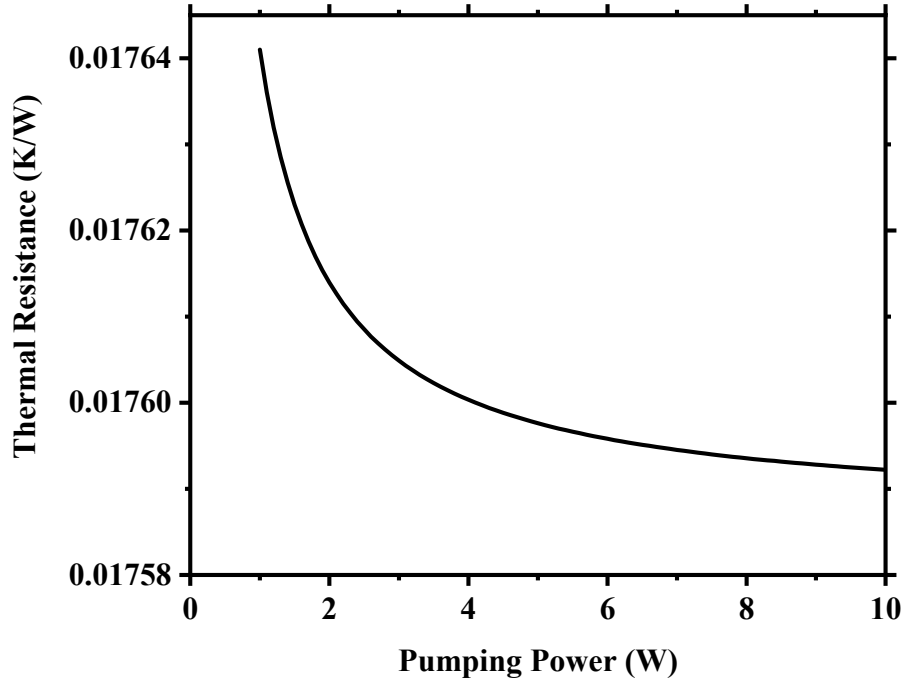

Figure 4. Thermal resistance vs. pumping power.

Figure 5 shows the relationship between the pumping power and the channel aspect ratio α at 50 °C. The pumping power is seen to increase with an increase in the channel aspect ratio. This behavior is consistent with the fact that a higher aspect ratio indicates a narrower channel, which requires an increase in pumping power for driving the coolant. Here, similar to the thermal resistance, the variation between the pumping power for the maximum and minimum pumping power is very small, i.e., 0.005%. The graph shows an exponential increase in pumping power for α values of one to four. After that, the pumping power becomes stable with a very slight increase.

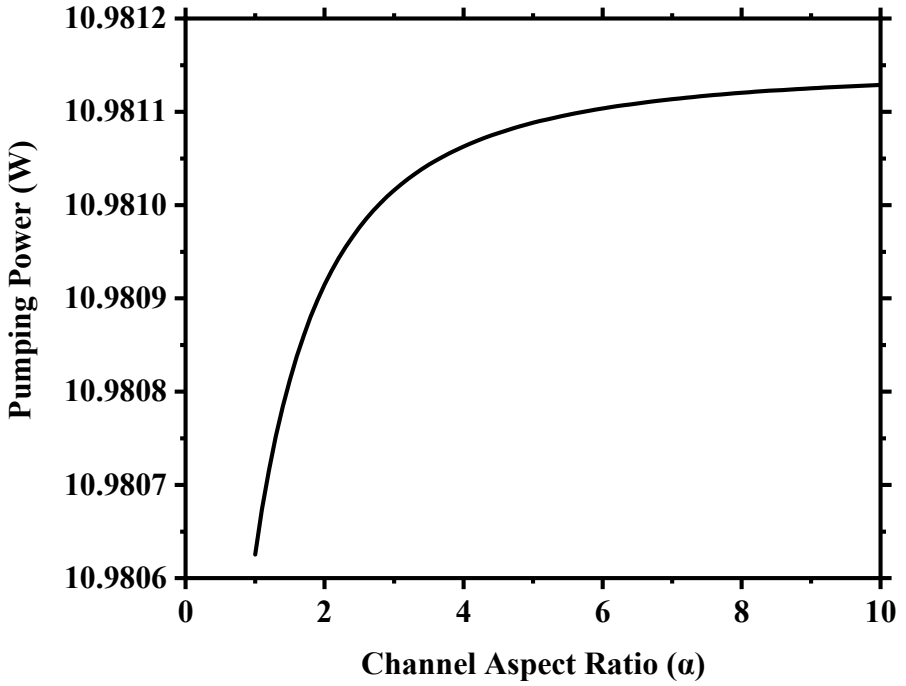

Figure 5. Pumping power vs. channel aspect ratio.

Figures 6 and 7 represent the variations in the thermal resistance and the pumping power, respectively, with respect to channel width ratio (β). Here, a higher width ratio signifies that the wall thickness of the channel is higher, meaning less availability of the flow area for the fluid. Like the variation of these parameters concerning channel aspect ratio (α), the differences between the different fluids are insignificant; thus, the results are only presented for water.

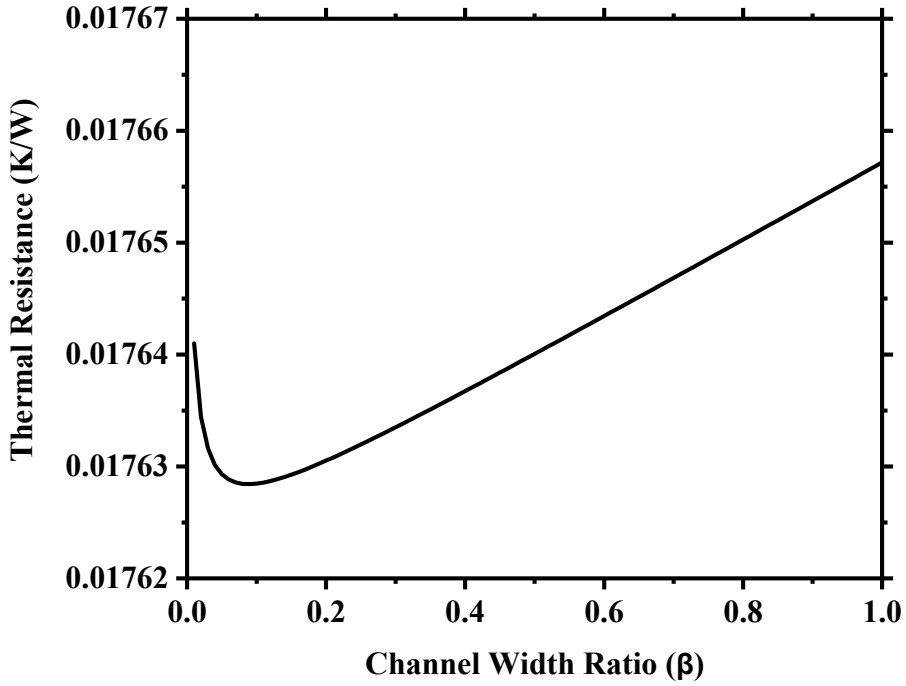

Figure 6. Thermal resistance vs. channel width ratio.

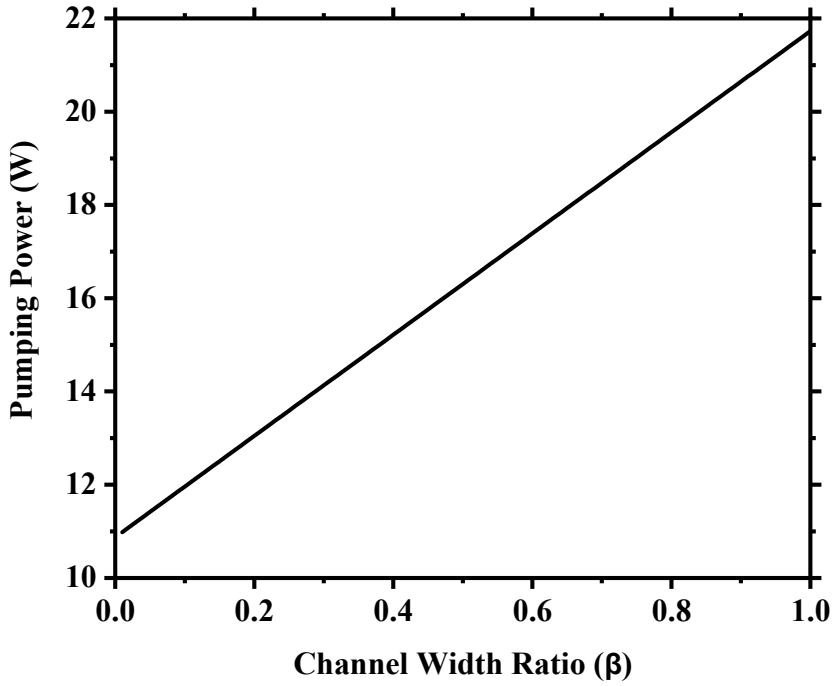

Figure 7. Pumping power vs. channel width ratio.

As shown in Figure 6, the variations in thermal resistance are exponential, similar to its variations with the channel aspect ratio (α). This is because a higher width ratio means

a lower area is available for the fluid flow, resulting in a greater mass flux and, thus, a higher Nusselt number. However, after a certain point, an increase in the mass flux does not reap benefits to the turbulent mixing of the fluid, resulting in less reduction in the thermal resistance beyond a certain point. This can be observed from the figure, where the reduction is significant until the channel width ratio is 0.05, but the reductions diminish beyond that point.

The reduction in the thermal resistance in this way comes at a heavy penalty in terms of pressure drop and, consequently, pumping power, as can be seen in Figure 7. As can be observed from the figure, the pumping power increases linearly with the increase in β. An increase of 9% in the pumping power is observed when β increases from 0.01 to 0.1 versus only a 0.1% reduction in the thermal resistance. This is the primary reason for the optimum channel width ratio being at its minimum value of 0.01.

4. Conclusions

A robust study of optimization of the MCHS is undertaken by using the MOMVO algorithm. In addition, six different fluids, consisting of water with varying proportions of nanoparticles, are used to study their effect on heat transfer enhancement. The channel aspect ratio and the channel width ratio are chosen as the design variables for the optimization algorithm. Thermal resistance and pumping power are chosen as the objective functions, which are minimized. Based on the study, the following conclusions are drawn.

- The optimization results using the MOMVO algorithm were found to be consistent when using different population sizes, enabling the use of a small population size to reduce the computational resources required.
- For the different fluids used in the study, the optimum performance is obtained for nanofluid with 0.01 weight concentration of nanoparticles in water.
- It is observed that the optimum solution obtained is skewed towards the x-axis (pumping power) instead of the x = y line, where it ideally should be. This indicates that the thermal resistance has a greater effect than the pumping power.
- Results show that the optimum channel width ratio is located at its lower bound. This is because a lower channel width ratio indicates that the channel is wider, and the walls are thinner, indicating a higher direct contact area for the fluid and the nearest part of the heat sink to the hot spot (bottom part in the present case), increasing the heat transfer. This follows the physics of fins, meaning it is not beneficial to put fins where the heat transfer coefficient is high.
- It is observed that the pumping power increases with an increase in channel aspect ratio. This is consistent with the physical phenomenon that an increase in channel aspect ratio results in a narrow channel, which requires higher pumping power.

This optimization algorithm can be utilized with other coolants that are being explored for better cooling performance. Such optimization techniques, coupled with experimental investigations, can contribute to completing the analysis of new potential coolants.

Funding: The author extends his appreciation to the Deputyship for Research and Innovation, "Ministry of Education" in Saudi Arabia, for funding this research (IFKSUOR3-046-3).

Data Availability Statement: Not applicable.

Conflicts of Interest: The author has no conflict of interest to declare.

Nomenclature

Nomenclature

$R_{thermal}$	Thermal resistance (°C/W)
$P_{pumping}$	Pumping power (W)
H	Height (m)
W	Width (m)
L	Length (m)

D	Diameter (m)
G	Mass flux (kg/m^2 s)
Re	Reynolds number
Nu	Nusselt number
k	Thermal conductivity (W/m K)
m	Mass flow rate (kg/s)
f	Friction factor
P	Pressure drop (Pa)
V	Velocity (m/s)
Subscripts	
c	Channel
h	Hydraulic
f	Fluid
av	Average
s	Solid
m	Mean
Greek Symbols	
α	Channel aspect ratio
β	Channel width ratio
ρ	Density (kg/m^3)
μ	Dynamic viscosity (Pa s)
Abbreviation	
MOMVO	Multi-objective multiverse optimisation
MCHS	Micro Channel Heat Sink
GA	Genetic Algorithm

References

1. Azar, K. Power consumption and generation in the electronics industry. A perspective. In Proceedings of the 16th Annual IEEE Semiconductor Thermal Measurement and Management Symposium (Cat. No. 00CH37068), San Jose, CA, USA, 23 March 2000; IEEE: Piscataway, NJ, USA; pp. 201–212.
2. Schaller, R.R. Moore's law: Past, present and future. *IEEE Spectr.* **1997**, *34*, 52–59. [CrossRef]
3. Wang, C.-C. A Quick Overview of Compact Air-Cooled Heat Sinks Applicable for Electronic Cooling—Recent Progress. *Inventions* **2017**, *2*, 5. [CrossRef]
4. Marcinichen, J.B.; Olivier, J.A.; Lamaison, N.; Thome, J.R. Advances in Electronics Cooling. *Heat Transf. Eng.* **2013**, *34*, 434–446. [CrossRef]
5. Maqbool, Z.; Hanief, M.; Parveez, M. Review on performance enhancement of phase change material based heat sinks in conjugation with thermal conductivity enhancers for electronic cooling. *J. Energy Storage* **2023**, *60*, 106591. [CrossRef]
6. Zhao, C.; Lu, T. Analysis of microchannel heat sinks for electronics cooling. *Int. J. Heat Mass Transf.* **2002**, *45*, 4857–4869. [CrossRef]
7. Kose, H.A.; Yildizeli, A.; Cadirci, S. Parametric study and optimization of microchannel heat sinks with various shapes. *Appl. Therm. Eng.* **2022**, *211*, 118368. [CrossRef]
8. Jing, D.; He, L. Numerical studies on the hydraulic and thermal performances of microchannels with different cross-sectional shapes. *Int. J. Heat Mass Transf.* **2019**, *143*, 118604. [CrossRef]
9. Ahmed, M.A.; Normah, M.G.; Ahmed, R. Thermal and hydrodynamic analysis of microchannel heat sinks: A review. *Renew. Sustain. Energy Rev.* **2013**, *21*, 614–622.
10. Ramos-Alvarado, B.; Li, P.; Liu, H.; Hernandez-Guerrero, A. CFD study of liquid-cooled heat sinks with microchannel flow field configurations for electronics, fuel cells, and concentrated solar cells. *Appl. Therm. Eng.* **2011**, *31*, 2494–2507. [CrossRef]
11. Saenen, T.; Baelmans, M. Numerical model of a two-phase microchannel heat sink electronics cooling system. *Int. J. Therm. Sci.* **2012**, *59*, 214–223. [CrossRef]
12. Harirchian, T.; Garimella, S.V. Microchannel size effects on local flow boiling heat transfer to a dielectric fluid. *Int. J. Heat Mass Transf.* **2008**, *51*, 3724–3735. [CrossRef]
13. Silvério, V.; Cardoso, S.; Gaspar, J.; Freitas, P.P.; Moreira, A. Design, fabrication and test of an integrated multi-microchannel heat sink for electronics cooling. *Sens. Actuators A Phys.* **2015**, *235*, 14–27. [CrossRef]
14. Kong, D.; Kim, Y.; Kang, M.; Song, E.; Hong, Y.; Kim, H.S.; Rah, K.J.; Gil Choi, H.; Agonafer, D.; Lee, H. A holistic approach to thermal-hydraulic design of 3D manifold microchannel heat sinks for energy-efficient cooling. *Case Stud. Therm. Eng.* **2021**, *28*, 101583. [CrossRef]
15. Nemati, H.; Moghimi, M.A.; Meyer, J.P. Shape optimization of wavy mini-channel heat sink. *Int. Commun. Heat Mass Transf.* **2021**, *122*, 105172. [CrossRef]
16. Yang, J.; Cheng, K.; Zhang, K.; Huang, C.; Huai, X. Numerical study on thermal and hydraulic performances of a hybrid manifold microchannel with bifurcations for electronics cooling. *Appl. Therm. Eng.* **2023**, *232*, 121099. [CrossRef]

17. Maghrabie, H.M.; Olabi, A.G.; Sayed, E.T.; Wilberforce, T.; Elsaid, K.; Doranehgard, M.H.; Abdelkareem, M.A. Microchannel heat sinks with nanofluids for cooling of electronic components: Performance enhancement, challenges, and limitations. *Therm. Sci. Eng. Prog.* **2022**, *37*, 101608. [CrossRef]
18. Zhang, Q.; Feng, Z.; Zhang, J.; Guo, F.; Huang, S.; Li, Z. Design of a mini-channel heat sink for high-heat-flux electronic devices. *Appl. Therm. Eng.* **2022**, *216*, 119053. [CrossRef]
19. Du, L.; Hu, W. An overview of heat transfer enhancement methods in microchannel heat sinks. *Chem. Eng. Sci.* **2023**, *280*, 119081. [CrossRef]
20. Shen, H.; Zhang, Z.; Ge, X.; Liu, H.; Xie, G.; Wang, C.C. Thermal analysis and experimental verification on double-layer microchannel heat sinks with impact jet nested arrays. *Int. J. Heat Mass Transf.* **2023**, *209*, 124169. [CrossRef]
21. Marshall, S.D.; Lee, P.S. 3D topology optimization of liquid-cooled microchannel heat sinks. *Therm. Sci. Eng. Prog.* **2022**, *33*, 101377. [CrossRef]
22. Ozguc, S.; Pan, L.; Weibel, J.A. Topological optimization of flow-shifting microchannel heat sinks. *Int. J. Heat Mass Transf.* **2023**, *207*, 123933. [CrossRef]
23. Shuqi, Z.; Limei, Y.; Goyal, V.; Alghanmi, S.; Alkhalifah, T.; Alkhalaf, S.; Alturise, F.; Ali, H.E.; Deifalla, A. Artificial neural net-work-based optimization of baffle geometries for maximized heat transfer efficiency in microchannel heat sinks. *Case Stud. Therm. Eng.* **2023**, *49*, 103331. [CrossRef]
24. Tan, P.; Liu, X.-H.; Cao, B.-W.; Chen, W.; Feng, J.-Y. Heat exchange mechanism analysis and structural parameter optimization for series-combined microchannel heat sinks. *Int. J. Therm. Sci.* **2023**, *187*, 108168. [CrossRef]
25. Ismail, O.A.; Ali, A.M.; Hassan, M.A.; Gamea, O. Geometric optimization of pin fins for enhanced cooling in a microchannel heat sink. *Int. J. Therm. Sci.* **2023**, *190*, 108321. [CrossRef]
26. Cui, H.C.; Shi, C.Y.; Yu, M.J.; Zhang, Z.K.; Liu, Z.C.; Liu, W. Optimal parameter design of a slot jet impingement/microchannel heat sink base on multi-objective optimization algorithm. *Appl. Therm. Eng.* **2023**, *227*, 120452. [CrossRef]
27. Bianco, N.; Fragnito, A.; Iasiello, M.; Mauro, G.M. Design of PCM-based heat sinks through topology optimization. *J. Phys. Conf. Ser.* **2023**, *2509*, 012001. [CrossRef]
28. Topin, M.F.; Lefevre, M.F.; Dendievel, M.R.; Vidal MP, E.; Bouvard, M.D.; Avenas, M.Y.; Ferrouillat, M.S. Modelling and Optimisation of Metal Foam Integrated Heat Sinks for Power Electronics Cooling. Ph.D. Thesis, University of Grenoble, Grenoble, France, 2021.
29. Shanmugam, M.; Maganti, L.S. Multi-objective optimization of parallel microchannel heat sink with inlet/outlet U, I, Z type manifold configuration by RSM and NSGA-II. *Int. J. Heat Mass Transf.* **2023**, *201*, 123641. [CrossRef]
30. Xiao, R.; Zhang, P.; Chen, L.; Zhang, Y.; Hou, Y. Experimental Study on Cooling Performance of a Hybrid Microchannel and Jet Impingement Heat Sink. *Appl. Sci.* **2022**, *12*, 13033. [CrossRef]
31. Abd Elaziz, M.; Oliva, D.; Ewees, A.A.; Xiong, S. Multi-level thresholding-based grey scale image segmentation using multi-objective multiverse optimizer. *Expert Syst. Appl.* **2019**, *125*, 112–129. [CrossRef]
32. Acharya, S.; Ganesan, S.; Kumar, D.V.; Subramanian, S. A multi-objective multiverse optimization algorithm for dynamic load dispatch problems. *Knowl.-Based Syst.* **2021**, *231*, 107411. [CrossRef]
33. Sundaram, A. Multiobjective multi verse optimization algorithm to solve dynamic economic emission dispatch problem with transmission loss prediction by an artificial neural network. *Appl. Soft Comput.* **2022**, *124*, 109021. [CrossRef]
34. Xu, W.; Yu, X. A multi-objective multiverse optimizer algorithm to solve environmental and economic dispatch. *Appl. Soft Comput.* **2023**, *146*, 110650. [CrossRef]
35. Loon, Y.W.; Sidik, N.A. A comprehensive review of recent progress of nanofluid in engineering application: Microchannel heat sink (MCHS). *J. Adv. Res. Appl. Sci. Eng. Technol.* **2022**, *28*, 1–25.
36. Gómez-Villarejo, R.; Aguilar, T.; Hamze, S.; Estellé, P.; Navas, J. Experimental analysis of water-based nanofluids using boron nitride nanotubes with improved thermal properties. *J. Mol. Liq.* **2018**, *277*, 93–103. [CrossRef]
37. Yusof, N.L.N.; Shamsuddin, H.S.; Estellé, P.; Mohd-Ghazali, N. Optimization of a boron nitride nanotubes nanofluid-cooled microchannel heat sink at different concentrations. *J. Therm. Anal. Calorim.* **2023**, *148*, 3117–3127. [CrossRef]
38. Cengel, Y.; Cimbala, J. *Ebook: Fluid Mechanics Fundamentals and Applications (SI Units)*; McGraw Hill: New York, NY, USA, 2013.
39. Cengel, Y.A. *Heat and Mass Transfer*; McGraw Hill Education: New York, NY, USA, 2011.
40. Shamsuddin, H.S.; Estellé, P.; Navas, J.; Mohd-Ghazali, N.; Mohamad, M. Effects of surfactant and nanofluid on the performance and optimization of a microchannel heat sink. *Int. J. Heat Mass Transf.* **2021**, *175*, 121336. [CrossRef]